

Solid-State NMR Study of the Multiphase Behavior of Linear and Cross-Linked Poly(1,3-dioxolane)

Filip E. Du Prez and Eric J. Goethals*

Polymer Chemistry Division, Department of Organic Chemistry, University of Ghent, Krijgslaan 281 S4bis, B-9000 Gent, Belgium

Peter J. Adriaenssens, Jan M. Gelan,* and Dirk J. M. Vanderzande

Institute for Materials Research, Limburg University, Universitaire Campus, Department SBG-Building D, B-3590 Diepenbeek, Belgium

Received September 19, 1995

ABSTRACT: The multiphase behavior of poly(1,3-dioxolane) (polyDXL) in linear and network forms as a function of molecular weight and cross-link density of the samples was investigated by high-resolution solid-state ^{13}C NMR. The ability to introduce two acrylate end groups and to control the molecular weight of the polymer provided a unique way to synthesize polyDXL networks with molecular weights varying from 4000 to 9000 between the cross-links. Besides an elastomeric phase and a crystalline phase, the existence of a third phase with intermediate molecular mobility could be shown for cross-linked polyDXL. This could be realized by making use of different techniques, such as $T_{1\rho\text{H}}$ studies at well-selected contact times and careful Lorentzian deconvolution of the acetal ^{13}C CP/MAS resonance lines. In these OCH_2O resonances, the peak of the interphase is situated around 96 ppm, at about the same chemical shift as that of the elastomeric phase, but it has a broader bandwidth due to increased spin diffusion. The crystalline component having the broadest bandwidth is positioned around 93.4 ppm. While the introduction of cross-links clearly is attributed to the development of an interphase, $T_{1\rho\text{H}}$ studies demonstrated that the limited molecular mobility of this phase is independent of the cross-link density of the samples. The presence of such a noncrystalline, immobile interphase between the crystalline and elastomeric regions could not be demonstrated for linear polyDXL with a molecular weight range of 4000–9000.

Introduction

It is well-known that the size and shape of the domains in semicrystalline polymer materials influence their physical and mechanical properties to a great extent.¹ A variety of techniques, such as differential scanning calorimetry (DSC), dynamic mechanical thermal analysis (DMTA), X-ray scattering, and visible light and electron microscopy, have been applied to investigate the distribution of the polymer components among the different phases. The size scale on which the domains can be analyzed depends on the technique used.

While a combination of these techniques can offer detailed information on the crystalline and amorphous fractions of semicrystalline polymers, solid-state high-resolution ^{13}C NMR also allows the investigation of the amorphous regions in semicrystalline polymers on a molecular scale. With this technique, it was found that crystallizable polymers such as polyethylene,² polypropylene,³ and polytetrahydrofuran (polyTHF)⁴ not only consist of a crystalline phase and an amorphous phase but also contain a crystalline–amorphous interphase characterized by a limited molecular mobility.

For the past few years, we have been investigating polymer networks containing crystallizable segments. In such materials, the chain flexibility is restricted by the cross-links, resulting in a decrease of crystallinity compared to that of the linear homologues. It seemed interesting to investigate such materials with solid-state ^{13}C NMR, not only to distinguish crystalline from noncrystalline domains but also to consider the existence of other domains, which could be related to a crystalline–amorphous interphase or to chain segments

close to the branching points of the networks and in which the polymer chains have an intermediate molecular mobility.

For this study, we used poly(1,3-dioxolane) (polyDXL). PolyDXL belongs to the family of polyacetals which are prepared by cationic ring-opening polymerization of the corresponding cyclic monomers.^{5–6} Polymers with controllable molecular weights and bearing functional groups on both polymer ends can be obtained.^{7–9} If these end groups are polymerizable functions, such as acrylate esters, the corresponding polymer networks, in which the molecular weight between the cross-links can be varied, are accessible by free radical polymerization.^{8,10}

PolyDXL is a semicrystalline polymer which has been studied by DSC and X-ray diffraction.^{11–13} From microscopic analysis, it was found that linear polyDXL, crystallized at temperatures higher than 22 °C, presents two crystalline phases. These phases are associated with two melting endotherms observed by DSC and are attributed to the formation of two different crystal structures.

In this study, solid-state ^{13}C NMR and, in particular, cross-polarization (CP) and cross-depolarization (CDP) combined with magic angle spinning (MAS) will be used to reveal the multiphase behavior of polyDXL. The study will focus on the influence of the molecular weight on the distribution of polyDXL over the different phases and on the differences of the solid-state ^{13}C NMR results obtained with linear and cross-linked polymer.

Experimental Section

Preparation of α,ω -Bis-acrylate-Terminated PolyDXL. The synthesis of polyDXL α,ω -bis-acrylate is based on the cationic ring-opening polymerization of DXL in the presence of methylenebis(oxyethyl acrylate) as a transfer agent. The

* Abstract published in *Advance ACS Abstracts*, April 15, 1996.

synthesis of the transfer agent is similar to the synthesis of methylenebis(oxyethyl methacrylate) described earlier.^{7,8} The polymerization occurs at room temperature in dichloromethane. In a two-necked flask provided with an inlet for dry nitrogen and a glass neck equipped with a rubber septum are mixed 4.41 mL of CH_2Cl_2 and 5.59 mL of dioxolane (80 mmol). Next, 9 μL (8×10^{-5} mol) of methyl trifluoromethanesulfonate as initiator and 0.305 mL (1.38 mmol) of the transfer agent are introduced by means of a syringe. After the mixture has been stirred for 12 h, 0.223 mL (1.6 mmol) of triethylamine is added to terminate the polymerization. The solution is poured into 100 mL of diethyl ether and cooled to -116°C by liquid nitrogen. The precipitated polymer is finally filtered off on a cooled glass filter. α,ω -Bis-acrylate-terminated polyDXL could be obtained with a number-average molecular weight (M_n) equal to 4100 and a yield of 80%. The molecular weight of the polymer could be varied by changing the ratio of initiator to transfer agent concentration. Two linear samples with $M_n = 4100$ and 9050, respectively, were prepared. The powders were dried several days under vacuum and crystallized at 20°C for 4 weeks in a dry atmosphere.

Network Synthesis. In 0.5 mL of toluene are dissolved 1.2 g of bis-acrylate-terminated polyDXL ($M_n = 4100$) and 10 mg (2.9×10^{-5} mmol) of (trimethylbenzoyl)diphenylphosphine oxide (TMBPO). The viscous solution is placed between two glass plates, kept at 1 mm distance by a silicone rubber ribbon, and held 10 min under the UV light (25 mW/cm^2) of a mercury lamp (365 nm). The samples are removed from the glass plates and dried under vacuum at 60°C for 24 h. Before the NMR measurements were made, the same crystallization procedure as for the linear samples was followed. The molecular weight between the cross-links (M_c) is determined by the choice of the molecular weight of the prepolymer.

NMR Studies. The solid-state ^{13}C NMR spectra were recorded at room temperature on a Varian XL-200 spectrometer operating at 50.3 MHz. Magic angle spinning was performed at 4.0 kHz, making use of ceramic Si_3N_4 rotors. The Hartmann–Hahn condition ($\omega_H = \gamma_H B_{1H} = \gamma_C B_{1C} = \omega_C$) for cross-polarization was fixed at 31 kHz using the aromatic signal of hexamethylbenzene. The chemical shift of this signal at 132.1 ppm from TMS was applied as a standard. For decoupling of the protons in the ^{13}C CP/MAS experiments, a power of 40 kHz was used. Routine cross-polarization measurements were performed using mixing times in the range of 50–9000 μs and 2 s recycle time after collection of the FID. In the single pulse sequence under magic angle conditions (^{13}C MAS spectra), a repetition time of 2.5 s was used.

A multipurpose pulse sequence¹⁴ was used for the selective determination of the proton spin–lattice relaxation times in the rotating frame ($T_{1\rho\text{H}}$) and of the specific carbon–proton cross-polarization time constants (T_{CH}) for the different phases. For the $T_{1\rho\text{H}}$ experiment, proper acquisition parameters were selected to produce CP/MAS spectra as a function of the spin-locking time in the proton channel. For the T_{CH} experiments, CDP/MAS spectra were generated as a function of the carbon–proton contact time.

DSC Measurements. The heat of fusion of the samples was obtained on a Perkin Elmer 7 provided with a thermal analysis controller TAC7/DX at a heating rate of 10°C/min . The melting point of polyDXL is in the range of 45 – 65°C , depending on the molecular weight and cross-link density of the samples.

Results and Discussion

MAS and CP/MAS NMR Spectra. The monomeric unit of polyDXL, $(\text{OCH}_2\text{OCH}_2\text{CH}_2)_n$, contains two kinds of carbon with a ratio of 2/1 and resonance lines at respectively 67.5 (OCH_2 peak) and 96.0 ppm (OCH_2O peak). The MAS ^{13}C NMR spectra are recorded at a rather short repetition time (2.5 s) in order to accentuate the more mobile phase due to its shorter ^{13}C T_1 time. As illustrated in Figure 1a, the MAS spectrum of a polyDXL network ($M_c = 4000$) shows only two rather sharp resonance lines for both kinds of carbons of the

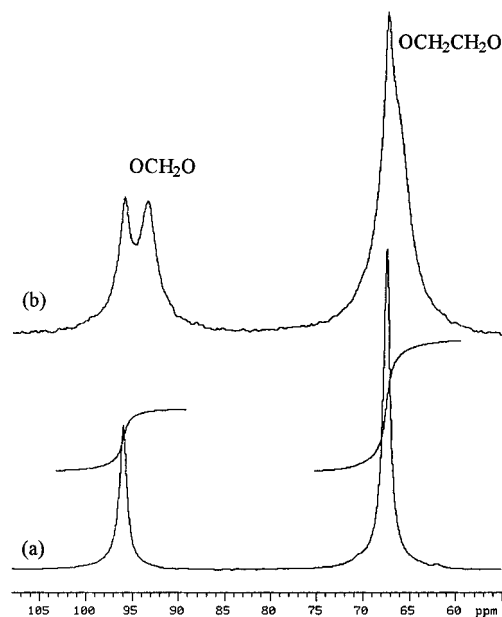


Figure 1. MAS (a) and CP/MAS (b) spectra of a polyDXL network ($M_c = 4000$).

polymer ($T_g = -50^\circ\text{C}$), similar to the liquid-state NMR spectra of the same polymer. On the contrary, the CP/MAS spectrum of the same network shows two peaks for each CH_2 group (Figure 1b). Due to the efficient cross-polarization of immobilized molecular units, a second peak appears at the upfield side for each CH_2 signal. It can be concluded that the OCH_2O resonance line for the elastomeric phase of the network is situated in the downfield peak at 96.0 ppm. The upfield peak at 93.4 ppm must be related to another less mobile phase of the polymer. A similar phase appearance is observed for the signal at 67.5 ppm of the $\text{OCH}_2\text{CH}_2\text{O}$ unit having a broad upfield shoulder around 66 ppm for the nonelastomeric phase.

Because of the semicrystallinity of polyDXL, the upfield peaks could be ascribed to the crystalline fraction of polyDXL. A more detailed peak assignment of the OCH_2O group in the CP/MAS spectra can be obtained by Lorentzian deconvolution of the overlapping signals (Figure 2). It reveals the presence of three peaks instead of two. One peak is situated around 96 ppm, with a liquid-like bandwidth of <1 ppm (45 Hz), corresponding to the elastomeric phase (E). A second peak, also situated around 96 ppm, has a broader bandwidth of about 2 ppm (110 Hz) and can be assigned to a less ordered interphase (I) which shows a reduced molecular mobility. A third peak is positioned around 93.4 ppm and has a bandwidth of about 3 ppm (140 Hz). It can be assigned to an ordered crystalline phase (C) which, of course, has also a reduced molecular mobility. The same peak positions and line widths for the three signals are confirmed by a series of 18 spectral deconvolutions of the corresponding OCH_2O signals of CP/MAS spectra at contact times varying from 50 to 5000 μs .

Dipolar line broadening in an interphase and in a crystalline phase, compared to the signals of an elastomer phase, can be understood on the basis of an increased spin exchange, induced by reduced molecular mobility, which results in shorter T_2 relaxation times. It must, however, be noted that the increasing crystalline fraction of the linear polymers and the networks with higher molecular weight between the cross-links

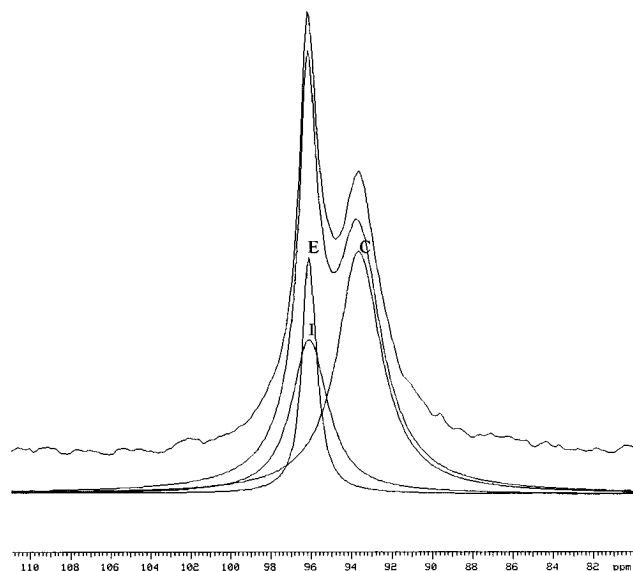


Figure 2. Lorentzian deconvolution of the CP/MAS spectrum (OCH_2O peak) of a polyDXL network ($M_c = 4000$), indicating the existence of a third component (I) besides the crystalline (C) and elastomeric (E) phases.

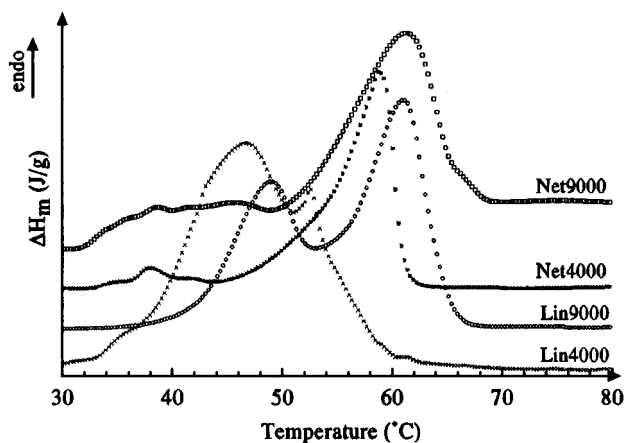


Figure 3. Heats of fusion versus temperature for polyDXL in linear and cross-linked forms. The samples are abbreviated as follows: Lin4000, linear polyDXL, $M_n = 4000$; Net4000, polyDXL network, $M_c = 4000$ (heating rate, $10^\circ\text{C}/\text{min}$).

appears in the CP/MAS spectra as a broadening of both resonance lines.

The line broadening in the crystalline phase could also be explained on the basis of the existence of two crystal forms, which was demonstrated by DSC measurements (Figure 3). Especially in the case of linear polyDXL, two endotherm peaks can clearly be observed. Each crystal morphology leads to a proper chemical environment for the carbons.

Magnetic Relaxation Behavior of PolyDXL. The presence of three different molecular environments can further be evidenced by analyzing the cross-polarization and the relaxation behavior of each phase. Therefore, the contact time (CT) in the standard CP/MAS experiment, during which the magnetization is transferred from ^1H to ^{13}C nuclei, is varied in the range of 50–9000 μs . Each phase reaches an optimal magnetization transfer at a certain contact time, depending on its molecular mobility and organization. A lower value of this optimal contact time corresponds to a smaller degree of molecular mobility in the phase at a certain temperature. This information can be used for the determination of the number of phases included in the

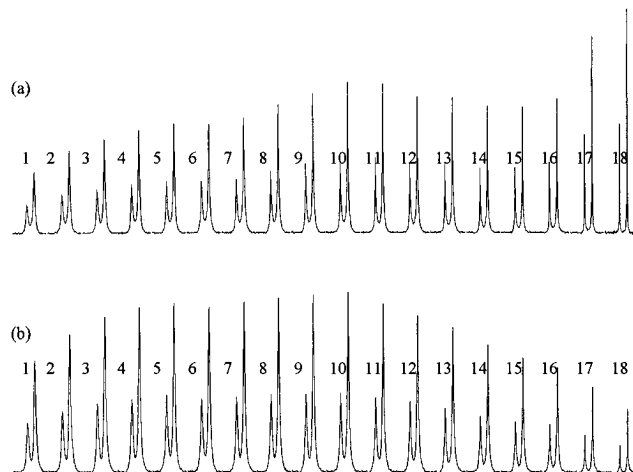


Figure 4. Contact time study of a polyDXL network ($M_c = 9000$) (a) and of linear polyDXL ($M_n = 9000$) (b), with CT varying from 50 to 9000 μs : 50 (1), 100 (2), 150 (3), 200 (4), 300 (5), 400 (6), 500 (7), 600 (8), 700 (9), 800 (10), 1000 (11), 1200 (12), 1500 (13), 2000 (14), 2500 (15), 3000 (16), 5000 (17), 8000 (18).

samples and for the estimation of the optimal contact time for each of the phases.

Such a contact time study is illustrated in Figure 4a for a polyDXL network ($M_c = 9000$). For the OCH_2O peak, as well as for the OCH_2 peak, three maxima, corresponding to the optimal contact time for each phase, can be distinguished at about 300, 800, and 8000 μs . Recognizing that a higher value of the optimal contact time corresponds to an increasing degree of mobility, the optima can be attributed respectively to an immobile crystalline phase, a nonordered interphase with limited molecular mobility, and an elastomeric phase with rubber-like mobility.

For networks with a smaller M_c value ($M_c = 4000$) (not shown), the CT optimum for the elastomeric phase shifts to a lower value (2000 μs), probably because the increased cross-link density reduces the elastomeric chain mobility. The CT optima for the two other phases remain respectively around 300 and 800 μs . The comparable crystalline behavior for both networks, as illustrated by the position of the melting peaks at approximately the same melting points in the DSC curves (Figure 3), could explain the identical optimal contact times for the crystalline phase of both networks.

Contact time studies were also done for polyDXL in linear form with different molecular weights. The analysis of such a study in Figure 4b demonstrates the presence of only two maxima at about 300 and 800 μs . Because of the absence of cross-links, there is an increased probability for crystallization. In comparison with the networks, the maxima can, therefore, be ascribed to the crystalline phase and to the interfacial region between the crystalline and the elastomer phase.¹⁵ Also, in the theory of Flory et al., such an interphase is described as a transition region, situated between the liquid-like elastomeric and the virtually perfectly ordered crystalline regions.¹⁶

The increased relative amount of the crystalline–elastomeric interphase in the networks could be explained on the basis of the introduction of chemical cross-links, resulting in the reduction of the length of the crystalline regions. The reduced mobility of the polymer chains near a cross-link, even in the molten state, hampers the polymer chains to be organized, resulting in a nonordered phase for which the mobility

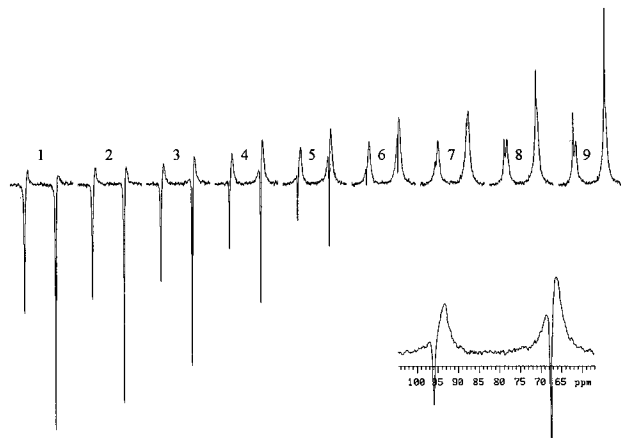


Figure 5. Cross-depolarization experiment of a polyDXL network ($M_c = 4000$) with different t_i values (in μs): 50 (1), 70 (2), 100 (3), 150 (4), 200 (5), 300 (6), 400 (7), 600 (8), 1000 (9). The spectrum at $t_i = 200 \mu\text{s}$ is given on the lower right.

can clearly be distinguished from that of the elastomeric phase.

Because of the higher degree of crystallinity in the linear polymers, and hence the reduced size and mobility of the elastomeric domains, the interphase and elastomeric phase cannot be detected separately anymore.

The existence of the multiphase behavior in a polyDXL network ($M_c = 4000$) can also be illustrated by a cross-depolarization (CDP/MAS) experiment with varying depolarization times (t_i). In this pulse sequence, the ^1H radio frequency transmitter phase is inverted after a fixed contact time, followed by a variable time t_i prior to carbon observation. During the evolution time t_i , carbon spins cross-polarize in the reversed direction. As a consequence, the carbon magnetization first decreases, vanishes at a certain moment, and finally increases along the opposite direction at a certain rate, depending on the cross-polarization efficiency for each phase. The evolution of the OCH_2O resonance line of a polyDXL network ($M_c = 4000$) at different t_i times is shown in Figure 5. The spectrum at $t_i = 200 \mu\text{s}$ is shown as an inset. It can be observed that the broader upfield peak at 93.4 ppm is already completely in the positive direction, while the sharp downfield peak at 96.0 ppm still appears in the negative direction due to the slower polarization transfer in the elastomeric phase. In this way, the CDP/MAS experiment allowed us to distinguish the elastomeric phase from the two other, less mobile phases, although the interphase and the crystalline phase could not be visualized separately.

Analysis of $T_{1\rho\text{H}}$ Relaxation Times of the Different Phases. The next step in the present work was to investigate the influences of the molecular weight in the linear polymers and of the cross-link density in the networks on the distribution of the different phases in polyDXL.

In a multiphase system, spin-lattice relaxation times in a rotating frame ($T_{1\rho}$) provide information on the microdomains involved in the spin system. Proton $T_{1\rho}$ values are sensitive to the motion of the ^1H system averaged out over a short distance because these $T_{1\rho\text{H}}$ relaxation times are determined by frequencies in the kilohertz frequency range, which reflect the motion of short segments in the polymer chain. The maximum diffusive path length L , over which proton-proton spin diffusion can occur, is approximately given by $L \approx (6DT_{1\rho\text{H}})^{1/2}$, where D is the spin diffusion coefficient ($\approx 10^{-16} \text{ m}^2/\text{s}$).¹⁷

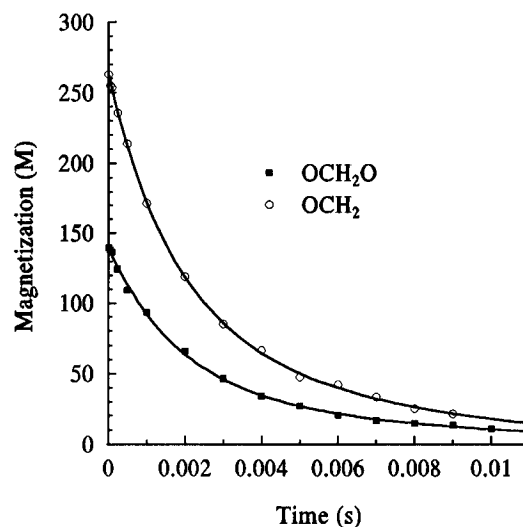


Figure 6. Magnetization of the methylene and ethylene carbon units of a polyDXL network with $M_c = 9000$ as a function of the evolution time t_i at a contact time equal to $800 \mu\text{s}$.

Multiple relaxation times will be observed only if the concerned phase sizes are larger than L and if the intrinsic relaxation times of the domains are sufficiently different at the experimental conditions used. In that case, $T_{1\rho\text{H}}$ values offer an interesting possibility to investigate the motional inhomogeneity of the samples and to estimate the minimum dimensions of the domains.

A full quantitative description of the $T_{1\rho\text{H}}$ CP/MAS experiment¹⁸ is too complicated for a polymer multiphase analysis. Therefore, the more simplified model of Aufla¹⁹ has been used after some adaptations. According to this model, the proton relaxation times in the rotating frame of each phase can be determined using the following adapted equation (CT = contact time):

$$M(t_e) = \sum M_0 \exp\left(-\frac{\text{CT} + t_e}{T_{1\rho\text{H}_i}}\right) \quad (1)$$

in which $M(t_e)$ corresponds to the overall magnetization as a function of the variable evolution time t_e . The subscript i refers to the concerned phase, later specified as C, I, and E for the crystalline phase, the interphase, and the elastomeric phase. The evolution time in eq 1 is extended with the contact time CT, during which $T_{1\rho\text{H}}$ relaxation already occurs.

In the $T_{1\rho\text{H}}$ experiments, evolution times (t_e) in the range of $10 \mu\text{s}$ to 0.01 s were used at the optimal contact times for each phase. Assuming that the magnetization of the other phases does not contribute to the overall magnetization at the optimal contact time of the investigated phase, the relaxation times of each phase could be investigated separately. However, a multiphase analysis by means of a curve-fitting program was mostly required. It must be emphasized that a baseline correction was implemented in the curve-fitting.

For example, in the case of the polyDXL network ($M_c = 9000$), three $T_{1\rho\text{H}}$ studies were performed at contact times respectively equal to 100, 800, and $6000 \mu\text{s}$. In each case, the area under both the OCH_2O and OCH_2 peaks was plotted as a function of the evolution time. As illustrated in Figure 6 at CT = $800 \mu\text{s}$, the above-mentioned network can be analyzed as a two-component system.

Table 1. $T_{1\rho H}$ Values (in ms) of the Different Phases in Linear and Cross-Linked PolyDXL for the Methylene and Ethylene Carbon Units

sample (χ_c) ^b	CT = 100 μ s				CT = 800 μ s				CT = 6000 μ s	
	OCH ₂ O		OCH ₂		OCH ₂ O		OCH ₂		OCH ₂ O	OCH ₂
	$T_{1\rho HC}$	$T_{1\rho HI}$	$T_{1\rho HC}$	$T_{1\rho HI}$	$T_{1\rho HC}$	$T_{1\rho HI}$	$T_{1\rho HC}$	$T_{1\rho HI}$	$T_{1\rho HE}$	$T_{1\rho HE}$
Lin4000 ^a (55%)	0.6	2.6	0.3	2.0	1.1	3.7	1.3	3.6	3.7	4.3
Lin9000 ^a (58%)	0.5	2.9	0.7	3.1	0.3	2.5	0.7	2.7	3.1	4.0
Net4000 ^a (29%)	1.0	3.5	0.6	2.0	0.2	2.5	0.9	2.5	7.1	5.7
Net9000 ^a (34%)	0.1	2.2	0.7	3.0	0.3	2.5	0.9	2.5	11.0	13.0

^a Lin 4000 and Lin9000 correspond to linear polyDXL with $M_n = 4000$ and 9000; Net4000 and Net9000 correspond to polyDXL networks with $M_c = 4000$ and 9000. ^b The values for the crystalline fraction (χ_c) are based on the melting enthalpy of 100% crystalline polyDXL, which is known to be 231 J/g.²⁰ Indium was used as calibration standard.

It is observed that, at higher contact times (e.g., CT = 6000 μ s), only the elastomeric part of eq 1 contributes to the overall magnetization, so that $T_{1\rho HE}$ can be determined separately from the two other relaxation times. On the contrary, at the lower contact times (100 and 800 μ s) for both the crystalline phase and the interphase, a two-component analysis was necessary to obtain a good curve fit. The $T_{1\rho H}$ values for the different phases thus estimated for both the OCH₂ and OCH₂O carbons are summarized in Table 1.

It can be concluded from Table 1 that the value of $T_{1\rho H}$ increases as the molecular mobility of the concerned phase increases (C < I < E). The systematic difference between the $T_{1\rho HC}$ and $T_{1\rho HI}$ values is a strong indication that the crystalline phase and the interphase can be regarded as separate molecular domains. On the other hand, the typical values of $T_{1\rho H}$ for the crystalline phase (± 1 ms) and the interphase (± 2.5 ms) remain the same for each sample within experimental error. This indicates that the degree of cross-linking or the molecular weight of polyDXL has no specific influence on the mobility of each of these two phases. It may seem surprising that one specific value has been obtained for each phase in the different samples, even if different crystal forms have been observed in the DSC spectra (Figure 3). This is, however, caused by rapid proton spin diffusion throughout the crystalline domains, resulting in similar $T_{1\rho HC}$ values.

Furthermore, two important pieces of information can be derived from the comparison of the $T_{1\rho HE}$ values in Table 1. First, increasing the molecular weight between the cross-links in networks results in higher values for these $T_{1\rho HE}$ relaxation times. This is due to the increasing molecular mobility of the elastomeric phase with decreasing cross-link density. For both networks, the values for $T_{1\rho HE}$ and $T_{1\rho HI}$ are clearly separated. The low crystalline fraction and the presence of immobile cross-links are two possible reasons for the existence of two noncrystalline phases.

Second, it can be observed that, for the linear polymers, the $T_{1\rho HE}$ values are close to the corresponding $T_{1\rho HI}$ values. Considering the experimental error as a consequence of the curve-fitting process, the differences between these values are negligibly small. In fact, although the same multiphase analysis procedure was followed as for the networks, i.e., the assumption of three distinguishable phases, the existence of a third phase in the linear samples could not be demonstrated, and the same conclusions after the contact time studies could be repeated here. Linear polymers allow a better organization of the polymer chain and hence lead to a higher fraction of the crystalline phase. In this low molecular weight range, the development of a mobile region in the middle of two crystalline regions is, therefore, strongly reduced.

The values of the $T_{1\rho H}$ relaxation time (3–4 ms) for the noncrystalline phase of the linear samples, near to the $T_{1\rho HI}$ values of the networks, justify the position of the second optimum (800 μ s) in the contact time study of linear polyDXL ($M_n = 9000$), being at the same position of the optimal contact time for the interphase in the polyDXL network ($M_c = 9000$) (Figure 4a).

Conclusion

High-resolution solid-state ¹³C NMR was applied for the investigation of the multiphase behavior of polyDXL in linear and network forms. It was demonstrated by three different methods that polyDXL in network form consists of three regions with increasing molecular mobility, respectively a crystalline phase, an interphase with limited molecular mobility, and an elastomeric phase. First, the presence of three peaks with different bandwidths could be observed in the CP/MAS spectra of these networks after a Lorentzian deconvolution of the OCH₂O signal. Second, cross-polarization contact time studies showed three maxima which correspond to the optimal contact times of three phases with a different degree of mobility. The existence of three phases was finally evidenced by $T_{1\rho H}$ studies at well-selected contact times. These results indicate that the introduction of cross-links on the one hand reduces the crystallization process, so that the probability of the development of a mobile phase increases, but on the other hand provides small regions where the polymer chains are intrinsically noncrystalline but immobile.

The values of the relaxation time in the rotating frame $T_{1\rho H}$ and the corresponding degrees of mobility for the crystalline phase and interphase are independent of the cross-link density of polyDXL. In contrast, the values of $T_{1\rho H}$ for the elastomeric phase strongly depend on the molecular weight between the cross-links, which is attributed to an increase of the mobility of this phase with decreasing cross-link density.

In the case of linear polyDXL, the presence of two noncrystalline phases, i.e., a mobile phase and an immobile phase, could not be demonstrated unambiguously by means of relaxation times. This is attributed to the absence of cross-links or to the better organization of the polymer chains in the crystalline lattice, which hampers the development of a mobile elastomeric phase, so that the noncrystalline phase is predominantly the one with a limited chain mobility.

Acknowledgment. F.E.D. is pleased to acknowledge support from the NFWO (Nationaal Fonds voor Wetenschappelijk Onderzoek). The "Federale Diensten voor Wetenschappelijke, Technische & Culturele Aangelegenheden" is acknowledged for financial support.

References and Notes

- (1) Utracki, L. A. In *Interpenetrating Polymer Networks*; Klempner, D., Sperling, L. H., Utracki, L. A., Eds.; Advances in Chemistry Series 239; American Chemical Society: Washington, DC, 1994; p 77.
- (2) Kitamaru, R.; Horii, F.; Murayama, K. *Macromolecules* **1986**, *19*, 636.
- (3) Saito, S.; Moteki, Y.; Nakagawa, M.; Horii, F.; Kitamaru, R. *Macromolecules* **1990**, *23*, 3256.
- (4) Hirai, A.; Horii, F.; Kitamaru, R.; Fatou, J. G.; Bello, A. *Macromolecules* **1990**, *23*, 2913.
- (5) Goethals, E. J.; De Clercq, R. R.; De Clercq, H. C.; Hartmann, P. J. *Makromol. Chem., Macromol. Symp.* **1991**, *47*, 151.
- (6) Schulz, R. C.; Hellermann, W.; Nienburg, J. In *Ring-opening Polymerization*; Ivin, K. J., Saegusa, T., Eds.; Elsevier: New York, 1985; p 369.
- (7) De Clercq, R. R.; Goethals, E. J. *Macromolecules* **1992**, *25* (3), 109.
- (8) Walraedt, S. R.; Goethals, E. J. *Polym. Int.* **1995**, *38*, 89.
- (9) Goethals, E. J.; De Clercq, R. R.; Walraedt, S. R. *J. Macromol. Sci., Pure Appl. Chem.* **1993**, *A30*, 679.
- (10) Du Prez, F. E.; Goethals, E. J. *Macromol. Chem. Phys.* **1995**, *196*, 903.
- (11) Alamo, R.; Fatou, J. G.; Guzmán, J. *Polymer* **1982**, *23*, 374.
- (12) Archambault, P.; Prud'homme, R. E. *J. Polym. Sci., Polym. Phys. Ed.* **1980**, *18*, 35.
- (13) Prud'homme, R. E. *J. Polym. Sci., Polym. Phys. Ed.* **1977**, *15*, 1619.
- (14) Hoogmartens, I.; Adriaenssens, P.; Vanderzande, D.; Gelan, J. *Anal. Chim. Acta* **1993**, *283*, 1025.
- (15) Kitamaru, R.; Horii, F. *Adv. Polym. Sci.* **1978**, *26*, 137.
- (16) Flory, P. J.; Yoon, D. Y.; Dill, K. A. *Macromolecules* **1984**, *17*, 862.
- (17) Douglas, D. C.; Jones, G. P. *J. Chem. Phys.* **1966**, *45*, 956.
- (18) Wu, X.; Zilm, K. W. *J. Magn. Reson. A* **1993**, *102*, 205.
- (19) Aufla, R. S.; Harris, R. K.; Packer, K. J.; Parameswaran, M.; Say, B. J.; Bunn, A.; Cudby, M. E. A. *Polym. Bull.* **1982**, *8*, 253.
- (20) Clegg, G. A.; Melia, T. P. *Polymer* **1969**, *10*, 912.

MA951404S